



SEISMIC HAZARD ANALYSIS OF MEXICO

FU WANG, CHRISTIAN P. MORTGAT, ZIFA WANG,
JANET L. BOLEY

Risk Management Solutions, Inc., Menlo Park, CA, 94025, USA

ABSTRACT

This study presents the results of a seismic hazard analysis for the country of Mexico. A probabilistic earthquake occurrence model was used in combination with seismic sources and ground motion attenuation to produce a seismic zonation map for the entire country. The phenomenon of ground motion amplification specific to the lake bed of Mexico City is addressed elsewhere. The seismicity of the segmented subduction zone off the west coast of Mexico was accounted for by a characteristic earthquake model for events above magnitude 6.8 M_s .

KEYWORDS

maximum magnitude, Mercalli intensity, Mexico, probabilistic hazard assessment, seismic sources, characteristic earthquakes, Poisson process model

INTRODUCTION

Mexico, located along the southwestern edge of the North American plate, is one of the most seismically active countries in the world. To the west, the northern portion of Mexico is bounded by the Pacific plate, while the southern and central regions are bordered by the Cocos plate and the Rivera microplate respectively. The Cocos and Rivera plates are moving towards Mexico in a northeast direction and are being forced, or subducted, beneath the overriding North American plate (Figure 1).

In the northern part of the subduction zone, roughly from Puerto Vallarta to Manzanillo, the Rivera plate is slowly subducting at a steep angle beneath the North American plate. Although the slow convergence rate leads to a correspondingly low seismicity level along this margin, at least six large earthquakes of magnitude greater than 7.0 have occurred in this zone since 1837.

Further south, approximately from Manzanillo to Tehuantepec, the Cocos plate is subducting more rapidly at a shallow angle which decreases southward. This region of the subduction zone is delineated by a series of sections or segments along the coast that cyclically generate large magnitude ($M > 6.8$) events with a frequency higher than in many other subduction zones around the world. These events have return periods as short as 30-40 years for some of the segments and usually display nearly identical rupture patterns and

magnitudes along the same portion of an individual segment or segments (extremely large events have been known to rupture several segments).

The Central Guerrero segment currently poses the highest potential hazard to Mexico City not only because of its proximity, but also because it has not experienced a major event since 1916. This segment has an average return period of 54 years for events of magnitude 6.8 or greater, thus it is well overdue for a large, damaging earthquake. Because of its seismic quiescence, this segment is commonly referred to as the 'Guerrero Gap'.

Historically, the segmented margin of the subduction zone has produced many damaging earthquakes. The destructive magnitude 8.1 Michoacán earthquake on September 19, 1985, was one such event. This tremor, the most damaging in Mexico's history, caused more than 10,000 deaths and 50,000 injuries in Mexico City while overall economic losses topped US\$ 4 billion. Other recent events along this margin include a magnitude 7.5 on January 30, 1973 on the coast of Michoacán, a magnitude 7.8 on November 29, 1978 in Oaxaca, and a magnitude 7.6 on March 14, 1979 near Petatlan which caused significant damage in Mexico City. Most recently, another characteristic event, a magnitude 7.6 on October 9, 1995 off the coast near Manzanillo, caused at least 44 deaths in the epicentral area.

South of Tehuantepec, the geometry of the subduction zone changes because the Cocos plate becomes much older and heavier, causing the subduction angle to become far steeper than in the north. This portion of the subduction zone has a lower seismicity rate than the northern region, although it is certainly not inactive.

A belt of shallow-focus intraplate earthquakes extends several hundred kilometers inland from the trench axis in southern central Mexico; the underlying tectonic mechanisms of these events are not well understood, and currently, there is no consensus among experts as to how to model these events. These shallow crustal earthquakes have very long return periods but can be extremely destructive because of their shallow depths. For example, a magnitude 7.8 shallow crustal event on January 3, 1920 between Veracruz and Puebla caused over 650 deaths in the epicentral area.

In the northern part of the country, the Pacific and North American plates move past one another along the northern extension of the East Pacific Rise, a transform boundary that bisects the Gulf of California and along which active sea-floor spreading is taking place. Though seismically active, the East Pacific Rise does not produce the damaging, high magnitude earthquakes generated in the subduction zone to the south.

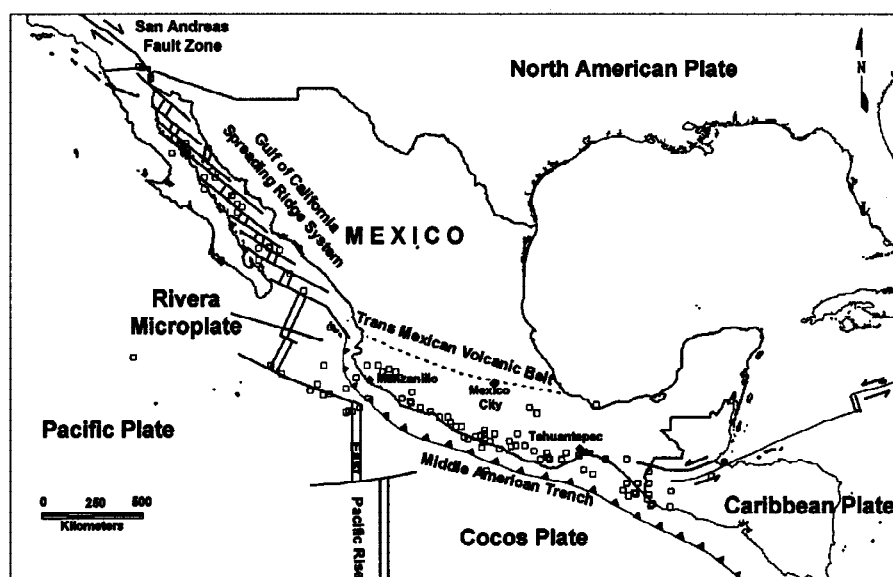


Fig. 1. Shallow seismicity (≤ 70 km) and major tectonic structures of Mexico. Earthquakes $M_s \geq 6.0$ from 1900-1993, PDE and NGDC catalogs.

In the California - Mexico border region, the East Pacific Rise transitions into the continental San Andreas Fault Zone in a series of shallow crustal faults. Also, west of the plate boundary, near the coastline and into northern Baja California, there are a series of west-northwest trending active strike-slip faults that are part of the larger southern California system of coastal and offshore faults.

This study examines the overall level of hazard across the entire country, analyzed probabilistically. The country-wide map was generated using standard probabilistic hazard analysis methods with a seismic source model described below. The resulting probabilistic map displays a measure of the level of hazard due to the contribution of all seismic sources.

EARTHQUAKE HAZARD MODEL

Seismic Source Zones and Recurrence Modeling

The RMS seismicity model for Mexico comprises four main source regions (Figure 2) which are discretized into individual source zones for hazard calculation purposes. The four main source regions are the Shallow Subduction Zone, the Inland Subduction Zone, the Gulf of California Seismic Zone and the Southern California Fault System.

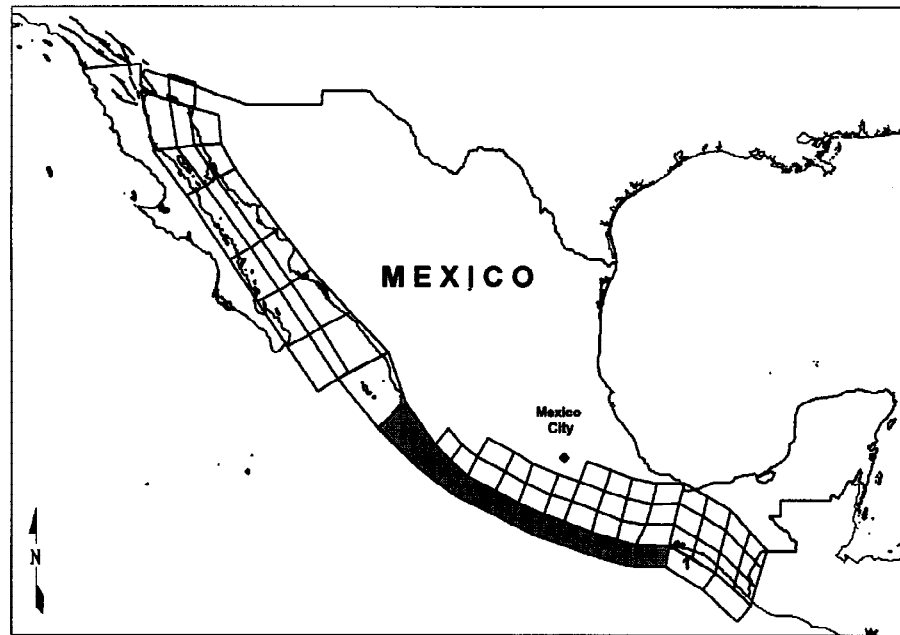


Fig. 2. Seismic sources used in the hazard model. Sources 2 -13 (shaded) employ the characteristic recurrence model.

Historical earthquake data were obtained from the NGDC catalog (Rinehart et al., 1982) and the PDE catalog (Rinehart et al., 1985) for the time periods 1900-1979 and 1945-1990 respectively. Duplicate events were removed, as well as aftershocks. The incompleteness of historical record with respect to magnitude was addressed by determining magnitude dependent time windows for which the record could be assumed reasonably complete. Additional epicenters were obtained from the database listed in Singh, Rodriguez, and Espindola (1984). The epicentral data for magnitudes $M_S \geq 6.0$ are plotted in Figure 1.

The earthquake occurrence in each source zone is described by the Gutenberg-Richter magnitude-frequency relation:

$$\ln N = \alpha + \beta M \quad (1)$$

where N is the annual number of earthquakes with magnitude greater than or equal to M , and α and β are constants. The Poisson process model was used to describe earthquake occurrence in time.

A. SUBDUCTION ZONE SOURCES

The Mexican subduction zone immediately adjacent to the Middle America Trench axis is broken out into 13 individual segments following the convention set forth in Nishenko and Singh, 1987. The characteristic earthquake model for the maximum event on each segment was adopted for all zones except the Tehuantepec Gap (Zone 1), which lacked sufficient data for analysis and was therefore modeled with the standard Gutenberg-Richter relationship.

The maximum magnitude of the characteristic event for each segment was determined using the relation developed by Heaton and Kanamori (1984):

$$M_w = (-0.00889)T + (0.134)V + 7.96 \quad (2)$$

where M_w is the maximum moment magnitude expected for a plate of age T (in millions of years) subducting at a relative velocity V (in centimeters/year).

The characteristic model adopted by RMS considers three magnitude ranges: 1) the upper magnitude interval ($M_2 - M_{\max}$) defined by the characteristic events, 2) events of magnitude up to M_1 characterized by the standard Gutenberg-Richter frequency-magnitude relation and 3) the magnitude interval between M_1 and M_2 with no seismicity (Figure 3, Table 1). The lower magnitude limit for the characteristic interval (M_2) was established by examination of the historic catalog of large and great earthquakes in each segment. The upper magnitude limit (M_1) for the Gutenberg-Richter relation was established through linear regression analysis of the historical epicenters located in the region.

The probability of occurrence of events of magnitude m or greater in a time period t is obtained as follows:

For $m < M_1$:

$$P = 1.0 - \exp[-[\exp(\alpha + \beta m) + N_{ch}] * t] \quad (3)$$

For $M_1 \leq m < M_2$:

$$P = 1.0 - \exp[-[(\frac{M_2 - m}{M_2 - M_1}) \exp(\alpha + \beta M_1) + N_{ch}] * t] \quad (4)$$

For $M_2 \leq m < M_{ch}$:

$$P = 1.0 - \exp[-[N_{ch} - \frac{(m - M_2)^2}{2T_1(M_{ch} - M_2)}] * t] \quad (5)$$

For $M_{ch} \leq m < M_3$:

$$P = 1.0 - \exp[-\frac{(M_3 - m)^2}{2T_1(M_3 - M_{ch})} * t] \quad (6)$$

For $M > M_{\max}$:

$$P = 0.0 \quad (7)$$

where:

M_{\max}	Maximum magnitude
M_1	Upper bound magnitude for G-R model
M_2	Lower bound magnitude for characteristic earthquake model
M_3	Upper bound magnitude for characteristic earthquake model
M_{ch}	Peak value for characteristic model triangular distribution

α, β	Gutenberg-Richter recurrence parameters alpha and beta
m	event magnitude
T_{ch}	return period for characteristic earthquakes
T	return period
T_1	$=T_{ch}(M_3-M_2)/2$
N_{ch}	$1/T_{ch}$ (occurrence rate of characteristic earthquakes)
t	time window
P	probability

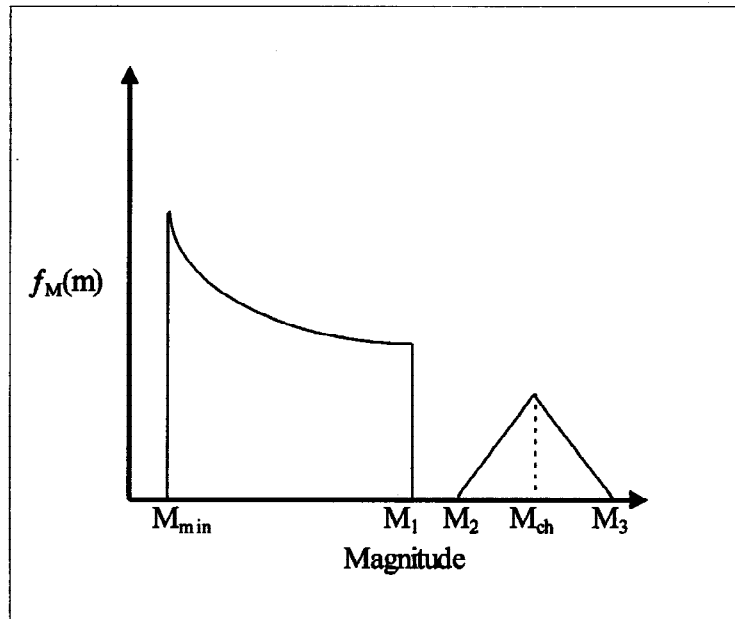


Fig. 3 Schematic diagram of combined Gutenberg-Richter frequency-magnitude relationship and triangular probability distribution for characteristic events used to model sources 2 - 13. Parameters are given in Table 1.

B. INLAND SUBDUCTION ZONE SOURCES

These sources are the inland continuation of the 13 subduction zone segments discussed in the previous section. They increase in depth (60 km to 120 km) to the east to accommodate the dip of the subduction zone. The zones are all modeled as area sources using the Gutenberg-Richter recurrence relation with maximum magnitudes estimated from the historical event catalog. The seismicity parameters for the sources were derived by performing linear regression analysis on the event catalog.

C. GULF OF CALIFORNIA SEISMIC SOURCES

These zones are shallow depth (12 - 15 km) sources which accommodate the seismicity of the spreading ridge system in the Gulf of California. The recurrence parameters of these sources were derived in the same manner as those of the inland subduction sources. It should be noted that the N. Jalisco zone, is a transitional zone that bridges the gap between the northernmost extent of the subduction zone and the southernmost portion of the spreading ridge system.

D. SOUTHERN CALIFORNIA FAULT SYSTEM SOURCES

A portion of these sources model the extension of the San Andreas Fault Zone within Mexico and accommodate the transition between a spreading ridge environment and a true transform boundary system.

Additionally, several faults along the coast of southern California are capable of generating damage in Mexico and were therefore included as well.

All of these zones are modeled as shallow depth (8 km) line sources reflecting surficially expressed faults in northern Mexico and southern California. All of these zones are modeled using the Gutenberg-Richter recurrence relationship with parameters derived in the same manner as for the non-characteristic model area sources.

Table 1. Maximum magnitudes (M_s), return periods for maximum events, and characteristic source parameters for sources 1 through 13.

No	Sourcename	Model	M_{max}	T_{ch}	M_1	M_2	M_3	M_{ch}	Depth (km)
1	Tehuantepec Gap	GR	8.4						40
2	E. Oaxaca	CH + GR	8.4	37	6.2	6.8	8.45	7.4	20
3	C. Oaxaca	CH + GR	8.4	54	6.2	6.8	8.45	7.4	20
4	W. Oaxaca 2	CH + GR	8.4	74	6.2	6.8	8.45	7.4	20
5	W. Oaxaca 1	CH + GR	8.4	38	6.2	6.8	8.45	7.4	20
6	Ometepec	CH + GR	8.4	39	6.7	6.8	8.45	7.4	20
7	San Marcos	CH + GR	8.4	57	6.7	6.8	8.45	7.4	20
8	C. Guerrero	CH + GR	8.4	54	6.7	6.8	8.45	7.4	20
9	Petatlan	CH + GR	8.3	36	6.2	6.8	8.45	7.4	20
10	Michoacan	CH + GR	8.3	74	6.2	6.8	8.45	7.4	20
11	Colima	CH + GR	8.3	32	6.2	6.8	8.45	7.4	20
12	Colima Gap	CH + GR	8.3	126	6.2	6.8	8.45	7.4	20
13	Jalisco	CH + GR	8.2	102	6.2	6.8	8.45	7.4	20

Ground Motion Attenuation

The PGA attenuation relationships for the model were adopted directly from Crouse (1991) for the subduction zone segments (sources 2 - 13), from Esteva and Villaverde (1973) for the inland subduction and Gulf of California sources and from Joyner and Boore (1988) for the San Andreas Fault system sources.

Both Esteva and Villaverde and Joyner and Boore include corrections to account for saturation effects at higher magnitudes. The three attenuations used and the source regions they apply to are as follows:

ESTEVA & VILLAVERDE:

$$PGA = 5.7 * \exp(0.8 * M) / (R + 40)^2$$

magnitude correction: if $M > 8.0$ then $M = 8.0 + (M - 8.0) / 2.0$

JOYNER & BOORE:

$$PGA = \exp[(-0.95 + 0.23 * M - \log_{10}(R) - 0.0027 * R) * 2.302]$$

magnitude correction: if $M > 7.0$ then $M = 7.0 + (M - 7.0) / 2.0$

CROUSE:

$$PGA = \exp[6.36 + 1.76M - 2.73 * \ln(R + 1.58 \exp(0.608M)) + 0.00916h] / 980.0$$

magnitude correction: none

where M is the M_s event magnitude, R is the hypocentral distance (km), h is the source depth (km), and PGA is the peak ground acceleration in cm/sec^2 .

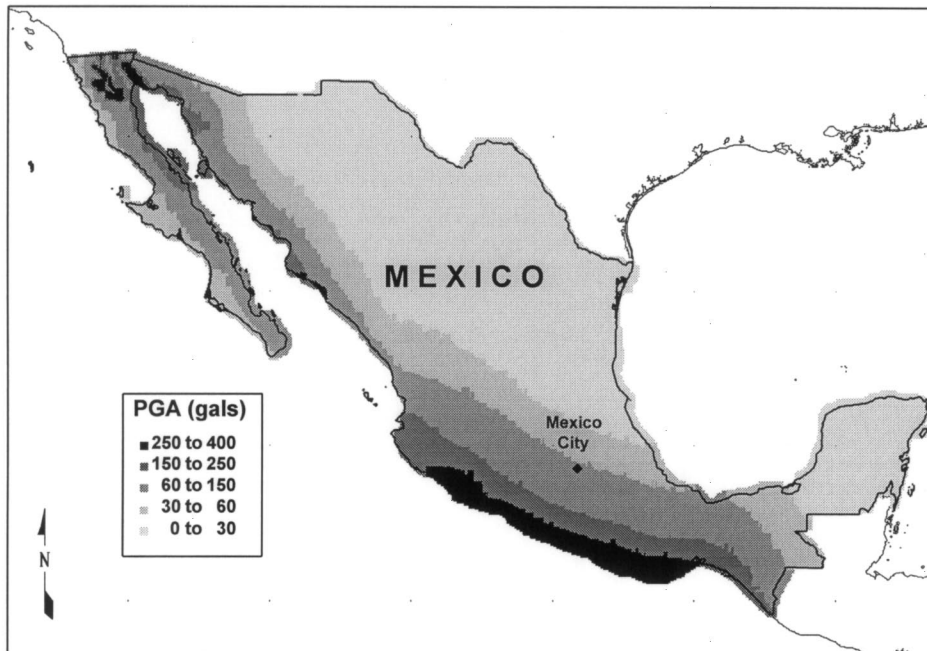


Fig. 4. Peak ground acceleration with a 10% probability of exceedance in 50 years.

In using the RMS source model to calculate a hazard map, the following assumptions were made:

- each area source was modeled as a series of line sources, with rupture length dependent on the event magnitude.
- event probabilities were evenly distributed among line segments in a source region.
- calculations were performed for best estimate quantities.

A seismic risk map showing intensities with 10% probability of exceedance in 50 years on average soil is presented in Figure 4. Within the RMS model, the cumulative effects of uncertainty from different sources, including the recurrence parameters and attenuation, are accounted for during calculation of building losses and do not readily lend themselves to display at the hazard level.

CONCLUSIONS

The primary goal of this study was to develop a model for use in seismic risk assessment. This model describes hazard from the primary seismogenic structures affecting the country of Mexico. When used in conjunction with building damage curves, inventory and soil hazard data specific to the country, it provides a tool for financial institutions and local planners to quantify potential losses to seismic hazards.

ACKNOWLEDGMENTS

We would like to thank Dr. Luis Esteva of the National University of Mexico (UNAM) for performing a critical review of the model. Mr. Paul VanderMarck and Dr. Pane Stojanovski at Risk Management Solutions, Inc. provided invaluable input during model development.

REFERENCES

- Anderson, J. G., S. K. Singh, J. M. Espindola and J. Yamamoto (1989). Seismic Strain Release in the Mexican Subduction Thrust. *Phys. Earth Planet. Inter.*, 58, 307-322.

- Crouse, C. B. (1991). Ground Motion Attenuation Equations for Earthquakes on the Cascadia Subduction Zone. *Earthquake Spectra*, 7, 201-236.
- Esteva, L. and R. Villaverde (1973). Seismic Risk, Design Spectra and Structural Reliability. In: *Proceedings of the 5th World Conference on Earthquake Engineering*, pp. 2586-2597. Rome.
- Heaton, T. H. and H. Kanamori (1984). Seismic Potential Associated with Subduction in the Northwestern United States. *Bull. Seism. Soc. Am.*, 74, 933-942.
- Joyner, W. B. and D. M. Boore (1988). Measurement, Characterization, and Prediction of Strong Ground Motion. In: *Proceedings of Earthquake Engineering & Soil Dynamics II*, GT Div/ASCE, Park City, Utah, June 27-30, 1988, pp. 43-102.
- McNally, K. C. (1981). Plate Subduction and Prediction of Earthquakes Along the Middle America Trench. In: *Earthquake Prediction - An International Review* (D. W. Simpson and P. G. Richards, eds.), Maurice Ewing Series, Vol. 4, American Geophysical Union, Washington, D.C.
- Nishenko, S. P., and S. K. Singh (1987). The Acapulco-Ometepec, Mexico, Earthquakes of 1907-1982: Evidence for a Variable Recurrence History. *Bull. Seism. Soc. Am.*, 77, 1359-1367.
- Nishenko, S. P., and S. K. Singh (1987). Conditional Probabilities for the Recurrence of Large and Great Interplate Earthquakes along the Mexican Subduction Zone. *Bull. Seism. Soc. Am.*, 77, 2095-2114.
- Ordaz, M. and S. K. Singh (1992). Source Spectra and Spectral Attenuation of Seismic Waves from Mexican Earthquakes and Evidence of Amplification in the Hill Zone of Mexico City. *Bull. Seism. Soc. Am.*, 82, 24-43.
- Rinehart, W., R. Ganse and P. Teik, National Geophysical Data Center (NGDC); Arnold, E. and C. Stover, U.S. Geological Survey (USGS); and Smith, R. H., (CIRES) (1982). *Seismicity of Middle America*. National Geophysical Data Center and National Earthquake Information Service, Boulder, Colorado.
- Rinehart, W., H. Meyers and C. A. vonHake (1985). Summary of earthquake data base. *Key to Geophysical Records Documentation No. 21*, U.S. Department of Commerce, National Geophysical Data Center, Boulder, Colorado.
- Singh, S. K. (1988). Analysis of historical seismograms of large Mexican earthquakes ($M_s \geq 7.0$): Summary of important results. In: *Historical Seismograms and Earthquakes of the World*, pp. 70-84. Academic Press, New York.
- Singh, S. K., L. Astiz and J. Havskov (1981). Seismic Gaps and Recurrence Periods of Large Earthquakes Along the Mexican Subduction Zone: A Reexamination. *Bull. Seism. Soc. Am.*, 71, 827-843.
- Singh, S. K., E. Mena and R. Castro (1988). Prediction of Peak, Horizontal Ground Motion Parameters in Mexico City from Coastal Earthquakes. *Geof. Int.*, 27, 111-129.
- Singh, S. K. and M. Pardo (1993). Geometry of the Benioff Zone and State of Stress in the Overriding Plate in Central Mexico. *Geoph. Res. Lett.*, 20, 1483-1486.
- Singh, S. K., M. Rodriguez and J. M. Espindola (1984). A Catalog of Shallow Earthquakes of Mexico from 1900 to 1981. *Bull. Seism. Soc. Am.*, 74, 267-279.